ELSEVIER

Precambrian Research 101 (2000) 87–109

Precambrian Research

www.elsevier.com/locate/precamres

Subaqueous eruption-fed density currents and their deposits

James D.L. White

Geology Department, University of Otago, PO Box 56, Dunedin, New Zealand

Abstract

Density currents fed directly from subaqueous eruptions can be divided conceptually into three groups based on modes of fragmentation and transport: (I) explosive fragmentation, with deposition from a gas-supported current; (II) explosive fragmentation, with deposition from a water-supported current; (III) fragmentation of flowing lava, with deposition from a water-supported current (Fig. 1). Group I products include subaqueously emplaced welded ignimbrite and other high-temperature emplaced subaqueous pyroclastic flow deposits. Group II products are the most varied, and include representatives of both high- and low-concentration turbidity currents, grainflows and debris flows, and are termed eruption-fed aqueous density currents. Some clasts in such currents are transported and even deposited at high temperature, but the transporting currents, ranging from grain flows to dilute turbidity currents, are water dominated even though steam may be developed along large clasts' margins. Group III products formed from lava flow-fed density currents tend to be weakly dispersed down-gradient along the seafloor, and generally consist largely of fragments formed by dynamo-thermal quenching and spalling. Bursting of bubbles formed by vapor expansion probably contributes to some Group III beds. Distinctive column-margin fall deposits may form in water-excluded zones that developed very locally around vents in association with Group I and II deposits, and are distinguished by heat retention structures, indicators of gas-phase transport and absence of current-formed depositional features.

Keywords: Density currents; Clasts; Seafloor; Pyroelastic fluids; Pyroelastlic density currents; Turbidity current

1. Introduction

A wide range of deposits consisting entirely of fresh volcanic fragments are formed by subaqueous density currents. Density currents bearing unmodified eruption-formed fragments originate both directly from volcanic eruptions (pyroclastic flows and surges) and indirectly by remobilization and redeposition of material initially emplaced by a different process (Fisher and Schmincke, 1984; Cas and Wright, 1987; McPhie et al., 1993). Different researchers apply different terms to redeposited tephra, but for subaerial settings there is agreement that primary pyroclastic deposits include all those formed as a result of eruptive fragmentation followed by single-stage transport through the ambient atmosphere. For subaqueous settings, however, even deposits formed by fragmentation followed by uninterrupted transport through the ambient water column have been commonly termed 'reworked' or 'redeposited' (Cas and Wright, 1987; McPhie et

E-mail address: james.white@otago.ac.nz (J.D.L. White)

0301-9268/00/$ - see front matter
PII: S0301-9268(99)00096-0

al., 1993), despite the absence of any 'unreworked' initial deposit. Though subaqueous eruption-fed deposits commonly involve water-supported transport, the transport and depositional processes are controlled by the nature of the eruption and its interaction with the surrounding water. Eruption-fed deposits should be distinguished wherever possible from genuinely reworked deposits, which may postdate an eruption by years or centuries, and which can provide far less information about the subaqueous eruptive process.

The aims of this paper are to review the various types of density currents generated by subaqueous eruptions, to outline the diagnostic features of resulting deposits and in particular those that can be applied to ancient rocks, and to assess the processes linking eruption style to transport and depositional processes.

2. Group I: subaqueous pyroclastic flows

The question of whether pyroclastic flows, which are high-temperature gas-solid flows (Aramaki, 1957; Aramaki and Yamasaki, 1963; Fisher and Schmincke, 1984), can occur subaqueously has been a contentious one (Sparks et al., 1980; Cas and Wright, 1991 and references therein), but paleomagnetic studies (Kano et al., 1994; Mandeville et al., 1994) and careful documentation of apparent welding textures (Kokelaar and Busby, 1992; Schneider et al., 1992; Fritz and Stillman, 1996; White and McPhie, 1997) continue to bolster the case for the process. Subaqueous flow of a gas-supported density current must be driven by the excess density of the current relative to water, and thus requires a very high particle concentration to overcome the low density of the continuous gas phase. Pumiceous flows must also have a

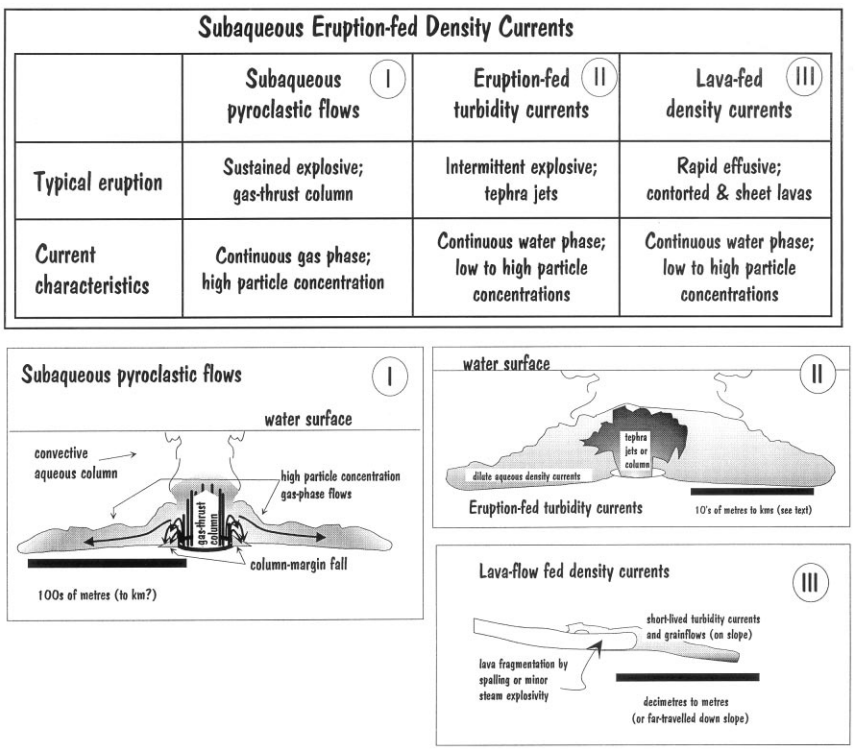

Fig. 1. Schematic summary of eruption-fed density current origins. (I) Explosively fragmented erupting magma feeds a hot, gas-supported subaqueous pyroclastic flow (note column-margin fall wedge at edge of vent in zone from which water is excluded by column gases); (II) explosively fragmented erupting magma feeds hot clasts into water-supported turbidity currents or granular flows; (III) fragmentation of flowing lava produces clasts entrained and distributed by small turbidity currents or granular flows.

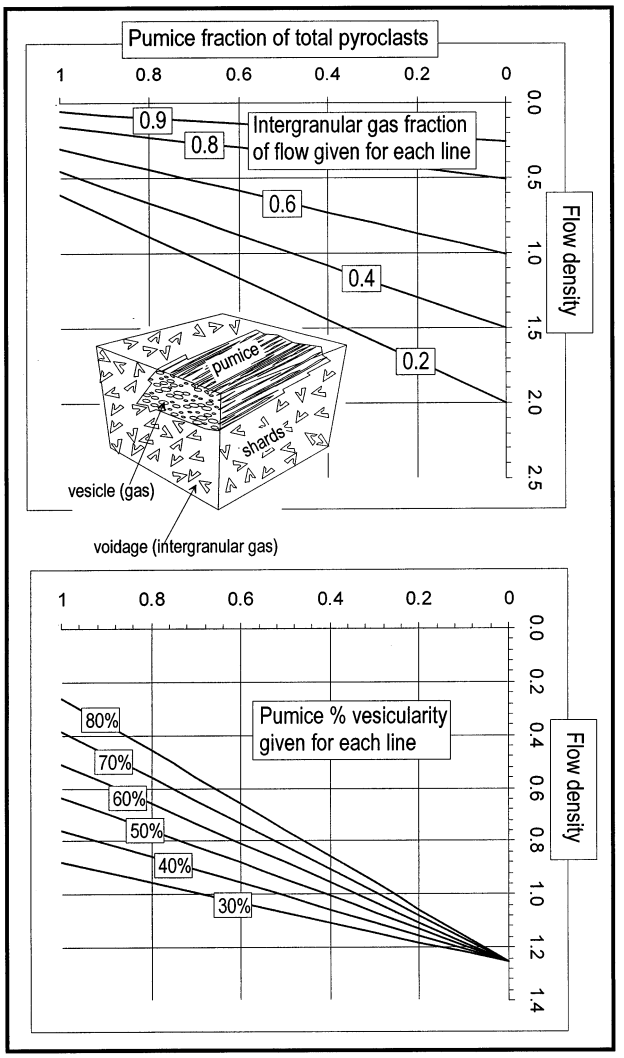

Fig. 2. (*Continued*)

large matrix-shard content to counteract the very low particle-density of pumice itself (Fig. 2). At such high particle concentrations grain support is likely to be by granular collision or hindered settling, though gas remains the continuous intergranular phase (Valentine, 1987; Branney and Kokelaar, 1992). This requires that the tephra travel as rigid, elastic particles (contrast Freundt and Schmincke, 1995), and implies that welding occurs only by post-depositional compaction within thick flow deposits. Sustained eruptions of strongly fragmented pyroclastic material from vents overlain by tens to hundreds of metres of water develop gas-thrust columns from which water is excluded (Kokelaar, 1983; Kokelaar and Busby, 1992). The heights of subaqueous gas-thrust columns are considerably suppressed because of the effect of hydrostatic confining pressure upon gas expansion, and pyroclastic flows fed from these suppressed columns are initiated with high particle concentrations. Flow interaction with the surrounding water is mediated by stripping of low-particle concentration zones from the top of the flow, and by a transient vapor barrier surrounding the main body of the flow and isolating it from surrounding seawater (Kokelaar and Busby, 1992; Fig. 3). Hydroplaning of high-concentration subaqueous flows (Mohrig et al., 1998) could result in localized, or under some circumstances extensive, disruption of the advancing pyroclastic flow front that may be represented by isolated bodies of tuff (Howells et al., 1985). Alternatively, the low excess densities (Fig. 2) of subaqueously initiated subaqueous pyroclastic flows may slow flow-front advance and inhibit hydroplaning.

Subaqueously erupted and deposited ignimbrite described by Busby-Spera (1986) and Kokelaar and Busby (1992) originally formed a massive,

Fig. 2. High particle concentration is necessary for subaqueous gas-supported flows. The two plots show variation in flow density as a function of pumice-shard ratio (shards are considered non-vesicular glass; glass density 2.5 gm/cm^3; gas density 0.01 gm/cm^3) plotted against (a) flow voidage (pumice vesicularity 70%), and (b) pumice vesicularity, for a flow with a voidage of 0.5 (flow consists by volume of 50% interstitial gas, 50% pumice + shards). Flow voidage ($\sim$ degree of expansion) has a much greater effect on flow density than does pumice vesicularity. The ratio of small non-vesicular shards to pumice is also very important. For instance at a voidage of 40% a mixture containing 70% pumice clasts will have a density of $\sim$0.75 gm/cm^3 (buoyant), whereas an ash-rich mixture consisting of 90% shards has a density of $\sim$1.75 gm/cm^3. Note that voidage levels greater than $\sim$0.6 are buoyant even when carrying only dense shards (no vesicles), and thus cannot flow beneath water. Voidage of 0.6 represents a very high-concentration current [e.g. fast granular flows (Campbell, 1990) cf. fluidized flows (Wilson, 1980)]: dilute currents commonly have voidage well above 0.999 [0.1% particles; (Freundt, 1998)], and a poorly sorted mixture at rest has voidage of around 0.2 (Nichols et al., 1994).

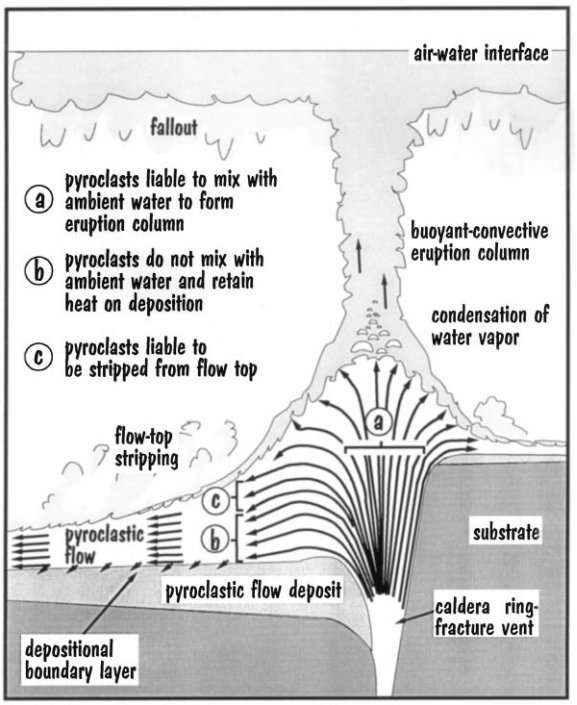

Fig. 3. Schematic diagram illustrates a subaqueous caldera-forming eruption producing a high-concentration particulate flow having gas as the inter-particle phase (after Kokelaar and Busby, 1992). Such flows form only from high-flux eruptions, and must have high particle concentrations to flow beneath water (Fig. 2).

unsorted deposit, up to c. 1 km thick in intra-caldera sites, passing laterally into thinner ignimbrite layers interstratified with water-settled tuff. Large blocks of country rock are present within the thickest and most massive deposits. Collapsed pumice fiamme form up to 50% of the rock, and visco-plastically deformed glass shards are pseudomorphically replaced by quartz–feldspar aggregates. The suite of deposits represents the subaqueous equivalent of a medium-volume ignimbrite forming Plinian eruption (Kokelaar and Busby, 1992). Similarly massive, pumiceous deposits with characteristics of subaerial ignimbrite and paleomagnetic evidence for high-temperature emplacement were deposited subaqueously during the Krakatau eruption (Mandeville et al., 1994).

Unwelded deposits of a gas-supported basaltic-andesite pyroclastic flow form a 5-m thick layer of non- to poorly stratified scoria lapilli tuff of Miocene age in Japan (Kano et al., 1994). Pumice swarms and gas-escape pipes occur locally, the base of the deposit has rip-up clasts and well developed load casts into underlying tuff, and the top of the layer grades into parallel laminated beds of basaltic-andesite tuff. Direct evidence for hot emplacement is provided by non-random thermoremanant magnetic orientations of scoria clasts. Hot emplacement is also suggested by strong load casting (from boiling of interstitial water in underlying tuff (Howells et al., 1985) and gas-escape pipes rooted at different levels within the deposit. Subaqueous deposition is supported by fossils in the enclosing sediment and an absence of shallow-water indicators.

There is a gradation between gas-supported and water-supported subaqueous density currents. Gas-supported flows may be transformed to water-supported ones by mixing along the length of a flow (Cas and Wright, 1991; Kokelaar and Busby, 1992). They may also grade with time into water-supported flows as a result of changes in eruption conditions (Mueller and White, 1992; Kano et al., 1996), as will be discussed below in connection with Group II deposits.

2.1. Recognition of Group I deposits

Diagnostic depositional features of subaqueous pyroclastic flows include, in addition to evidence from enclosing beds of continuous subaqueous depositional setting, welding textures, evidence of heat retention such as welding textures (Schneider et al., 1992) and, for younger deposits which have never been recrystallized, poor sorting and massive nature, and clasts with aligned thermoremanent magnetic orientations, together with poor sorting and massive nature (Table 1). Associated features are overlying co-genetic tuffs showing evidence for deposition from turbidity currents and subsequent suspension, and loading induced soft-state deformation of underlying sediments. Cold subaqueous pyroclastic flows should not exist because there is no mechanism for cooling the vent-derived interstitial gas without either expanding the flow to densities too low to flow beneath water, or ingesting water.

In studies of ancient rocks, particularly fossil-free deposits of Precambrian age, the existence of pre- and post-ignimbrite marine conditions may be best shown by presence of iron formation, turbidites, or tempestites. Wave indicators offer only ambiguous support because of the possibility of tens of metres of pre-eruption inflation and emergence preceding large silicic eruptions (Orton, 1991). Hot but unwelded pyroclastic-flow deposits probably cannot be unambiguously identified in the absence of a reliable paleomagnetic signature.

3. Group II: eruption-fed aqueous density currents

The group of subaqueous flows here grouped as eruption-fed aqueous density currents comprises dilute to high-concentration particulate gravity flows having water as the continuous intergranular phase. Most involve turbulence as a particle support mechanism, though vertical and/or lateral segregation may result in vertically stratified or laterally evolving currents in which parts of the flow are dominated by intergranular collisions and hindered settling. Individual clasts within such flows may remain hot during transport and deposition, but sufficient gas to exclude water from the bulk of the flowing mass is neither generated nor entrained during column collapse.

The classic 'doubly graded sequences' of the Tokiwa Formation (Fiske and Matsuda, 1964) are excellent examples of deposits from eruption-fed aqueous density currents as defined here. The deposits are over- and underlain by fossiliferous sub-wavebase marine deposits, and comprise extensive nonwelded lapilli tuffs and tuff breccias in beds from a few metres to several tens of metres thick. Tuff and lapilli tuff consists of glassy juvenile clasts ranging in vesicularity from dense to pumiceous, together with crystals of plagioclase and quartz. Fiske and Matsuda (1964) recognized a consistent association of thick, internally unstratified beds formed of larger clasts graded by fall velocity together with a finer sand-grade interstitial ash, overlain by thin, turbiditic beds consisting entirely of sand-grade ash. The thin beds show little size grading, but strong density grading marked by upward enrichment in pumice. A thinning and fining upward set of these thin beds, together with the underlying thick and unstratified bed, represents deposits of density flows fed from a single eruption. The authors viewed the eruption as having proceeded from gradual expansion of an eruption column into which water was ingested, to subsidence and outward flow of the bulk of this material in a water supported 'pyroclastic flow' (Fiske, 1963; Fiske and Matsuda, 1964, p. 84) to form the thick lower bed, to subsequent decay of dilute regions of the aqueous convective column to form a series of increasingly fine-grained and low volume turbidity current deposits. Water-supported 'pyroclastic flows' are terminological hybrids (Cas and Wright, 1991), and can be viewed instead as eruption-fed high-concentration aqueous sediment gravity flows that are either high-concentration turbidity currents and basal layers thereof (Lowe, 1982; Postma et al., 1988; Kneller and Branney, 1995; Sohn, 1997), or cohesionless debris flows or grain flows (Lowe, 1976; Postma, 1986; Nemec, 1990). The eruptions envisaged by Fiske and Matsuda (1964) involved

Table 1
Summary information for subaqueous pyroclastic flow deposits (Group I)

Feature	Inference	Interpretation
Fine grainsize	Efficient fragmentation	Explosive eruption
Massive, unsorted body of deposit	Deposition en masse or by continuous aggradation from over-capacity current	Deposited from high particle-concentration flow
Matrix welding	All fragments deposited hot	Passage from vent to depositional site without encountering water (steam-bordered column and flow)
Bedded, graded unwelded top	Traction deposition, multiple flows or pulses	Deposited from dilute aqueous currents carrying particles stripped from flow top

strong magmatic fragmentation at the vent, but were insufficiently vigorous and sustained to produce 'true' pyroclastic flows in which gas formed the continuous interparticle phase. The Tokiwa flows originated as the tephra particles were 'delivered' directly into the water column by eruptive processes. It is inferred here that tephra leaving the condensing or water-entraining margin of the gas-thrust region of the subaqueous eruption column became entrained as a population of discrete clasts into initially bouyant heated water, which upon cooling and sediment loading subsided and moved away from the vent as moderately dense sediment gravity flows. Additional coarse tephra dispersed through the water column may have continuously rained into the flows, suppressing any tendency to form distinct thin layering (Lowe, 1988; Arnott and Hand, 1989).

Archean deposits within the Hunter Mine Group represent an important variation in eruption-fed aqueous density current sequences, illustrating the gradational relationship of these flows to gas-supported subaqueous pyroclastic flows. Mueller and White (1992) described a continuous sequence of beds ranging from a massive lower unit in which large juvenile rhyolite clasts show evidence for soft-state deformation upon deposition, stratigraphically upward to thin beds of blocky rhyolite clasts (Fig. 4). A fountaining style of eruption is inferred on the basis of fluidally shaped clasts (Mueller and White, 1992). The ability of the clasts to retain heat during transport to the depositional site indicates isolation from surrounding water. Because fountaining eruptions are typified by efficient separation of particles from expanding volatiles at the vent (Head and Wilson, 1989), the exclusion of water from part of the eruption-fed current is ascribed to generation of steam where outer parts of thea high-concentration density current (debris-flow or fast granular flow) dominated by closely-spaced high-temperature clasts encountered and transferred heat to water. This mode of steam generation is attritional, because flow-margin clasts are cooled and fragmented in the process of forming the steam which isolates more inward parts of the flow from surrounding water. The non-welded nature of the matrix to the large clasts in the upper part of the lower unit indicates that the current changed with time. Initially, the steam generated as heat was transferred from the closely spaced particles caused water to be almost entirely displaced from lower parts of the depositing current. Upwards in the deposit and with time, the current became one in which water was the continuous phase yet in which the larger clasts remained insulated by self-generated steam jackets, persisting because of the greater heat content of the large clasts. The eruption itself evolved from a dense suppressed magmatic fountain to a phreatomagmatic eruption in which particle fragmentation was in part driven by water entering the vent and the pyroclasts were carried upward convectively entrained in an aqueous column (Fig. 4).

Subaqueously formed deposits of Pahvant Butte volcano, which grew within Lake Bonneville during the late Pleistocene (Gilbert, 1890), illustrate the importance of eruption style in determining the style of resulting sediment-gravity flows (White, 1996). A broad mound of shallow-dipping ($< 5°$) tephra beds was built during the subaqueous phase of eruption at Pahvant Butte, reflecting efficient outward transport of debris by the eruption-fed subaqueous currents. Beds forming the bulk of the mound are relatively thin and show a variety of tractional current structures such as scours and cross-lamination (Fig. 5a–c). It is inferred that these beds reflect deposition from numerous dilute gravity currents with tractional flow-boundary zones, each fed by a discrete eruptive pulse (White, 1996). The pulses are equivalent to the intermittent tephra jets observed subaerially during the eruption of Surtsey (Thorarinsson, 1967), but when occurring entirely subaqueously the steam in the jets rapidly condenses, leaving concentrations of pyroclasts from the jets suspended in the water column. The pyroclast suspensions transform to vertical gravity currents that impinge on the lake floor and then flow both back toward the vent and away from it to form the broad low relief platform. Subsequent pulses initiated before deposition from a preceding current is complete will pass shock waves through the moving currents, and temporarily inhibit ventward flow (Figs. 6 and 7a–b). The dispersion of

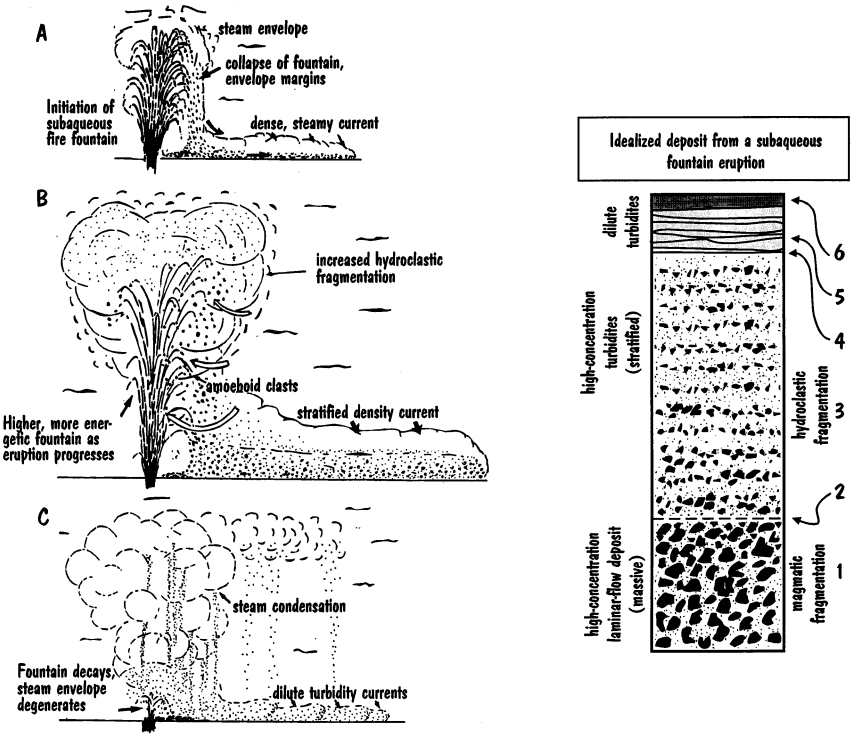

Fig. 4. Schematic model (left) of a subaqueous fire-fountain eruption (after Mueller and White, 1992). (A) Erupting fluid magma is torn apart by magmatic gas expansion in the fountain, is largely enclosed within a steam envelope; spatter-like amoeboid clasts are formed. Marginal fountain subsidence produces dense, lateral flows of amoeboid clasts within a steam-rich matrix: these flows produce initially hot deposits in which amoeboid clasts continue to deform, becoming locally pressed together. (B) Fountain becomes more strongly affected by hydrovolcanic processes as the eruption progresses, turbulence at the boundaries of the steam envelope causing increasing ingestion of water into the fountain and increasing turbulence at the margin. Water entering the fountain causes abrupt cooling and hydroclastic fragmentation of the erupting magma in much of the fountain, but parts remain isolated from ingested water and continue to produce amoeboid clasts. Particulate density flows shed from the fountain margins move away from the vent as stratified high-concentration sediment gravity flows. Amoeboid clasts entrained in these flows are preserved against hydroclastic fragmentation by steam generated along the margins of the clasts themselves during transport. Unlike amoeboid clasts deposited from early fountain collapse, these are cooled before deposition and do not weld together. (C) As the eruption wanes and magma volume flux decreases, the fountain progressively condenses and disintegrates, forming a series of increasingly dilute pyroclastic turbidity currents, which deposit a succession of variably thick Bouma turbidites. Remaining fine-grained ash is carried away from the eruption site to form more widespread subaqueous fallout deposits. Simplified stratigraphy (right) of pyroclastic deposits produced by one eruption event. (1) Massive deposit with hot-emplaced amoeboid clasts. (2) Diffuse contact. (3) Matrix-rich and matrix-poor layers with predominantly blocky, hydroclastically fragmented, grains. (4) Sharp contact. (5) Deposits of dilute turbidity currents with low-angle scouring and truncation. (6) Rapid post-eruption suspension deposit (aqueous fall) overlain by iron formation.

particles initially forming the sediment gravity flows represents a critical distinction from otherwise similar flows originating by sediment failure on steep slopes that must evolve from debris flows by ingestion of water (Sohn et al., 1997). Dilute eruption-fed flows likely evolve as waning, depletive turbidity currents, and may uniquely lack an initial waxing, accumulative phase (Kneller and Branney, 1995).

A variant of this process becomes active as the mound shoals to near lake level, and involves interaction of the density currents with surface waves. Resulting combined-flow deposits are characterized by low, broad duneforms, vaguely similar to those of low-particle concentration steam-poor pyroclastic surges (Wohletz and Sheri-

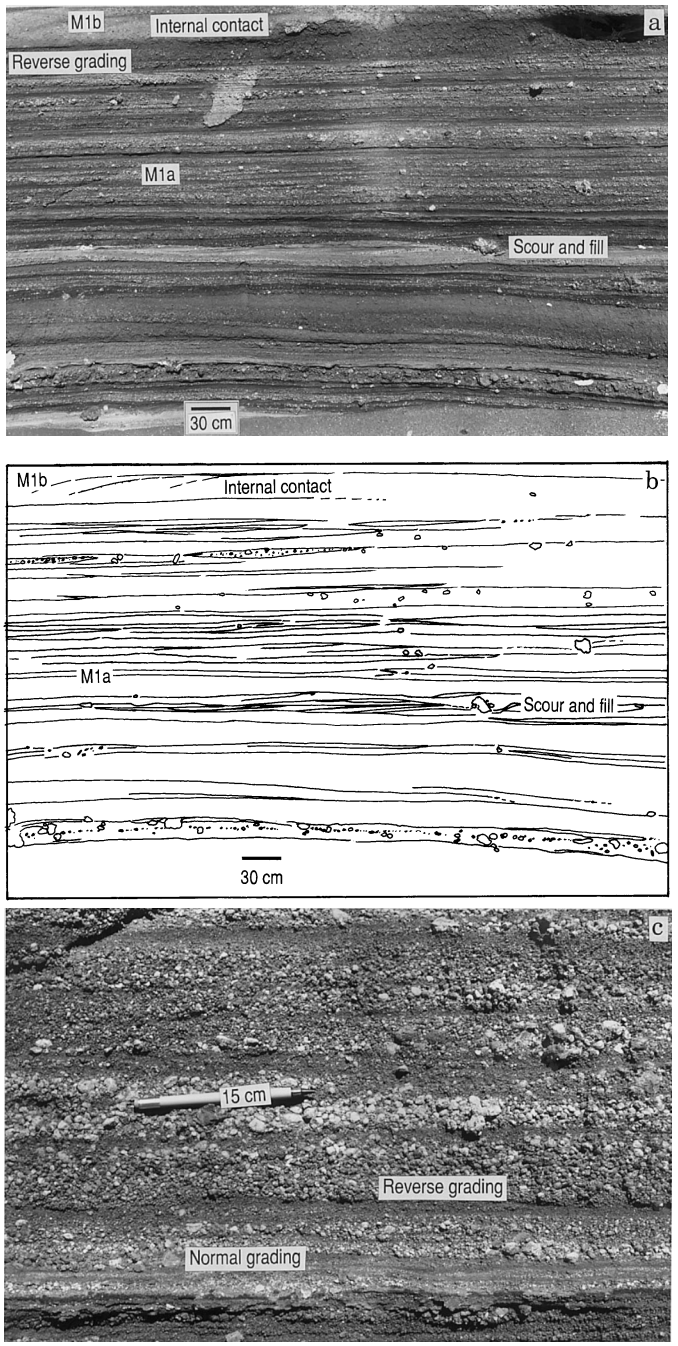

Fig. 5. Bedding characteristics of Pahvant Butte mound strata. Illustrated lithofacies are (a–b) Typical subhorizontal, very subtly lenticular bedding of M1a lithofacies. The reverse-graded base and vague internal contacts are visible in an M1b bed near the top. Note scour and fill associated with outsized clast on right side of photo. (c) Detail of M1a bedding showing low-angle scouring, normally graded layers, reverse-graded layers, cross-stratification and lateral grain-size variation in single layers (pencil) is 15 cm long. (d–e) Pervasive low-angle lenticularity and sweeping truncation surfaces typify lithofacies M3. Thicker structureless or subtly stratified beds are stippled on drawing from the photo. Vertical line marks edge of area in drawing. (f–g) High- to low-angle cross-strata in M3. Note low angle cross-stratification in sigmoidal duneforms, and concentration of lapilli at toes of cross strata (arrow). Bedding surfaces descend gently to the left, outward and downcurrent from the vent (after White, 1996).

dan, 1983), which increase in development and abundance upward in the mound sequence (Fig. 5d–g and Fig. 7c).

Thin, shallow-dipping tephra beds also make up the subaqueously formed mound-shaped volcano of Black Point (Fig. 8), on the shore of

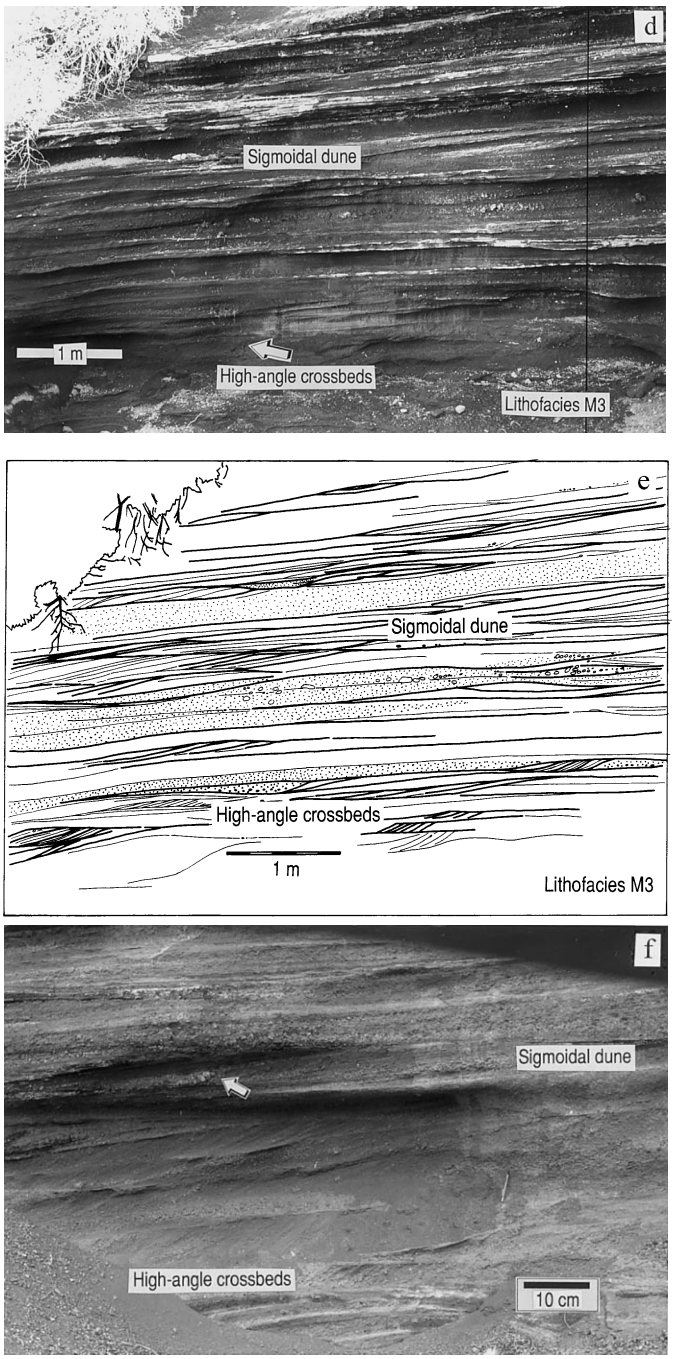

Fig. 5. (*Continued*)

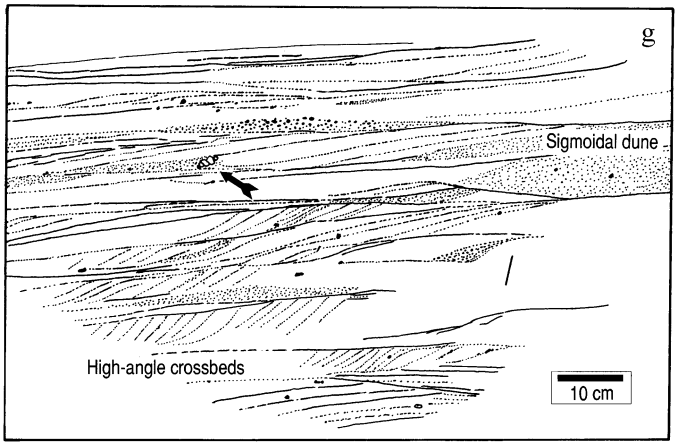

Fig. 5. (*Continued*)

Mono Lake, California (Christensen and Gilbert, 1964; Custer, 1973; White, 1994). The mound comprises c. 100 m of moderately well sorted coarse ash and lapilli in beds centimeters to decimeters thick (Fig. 9a–d), generally similar to the mound strata at Pahvant Butte. Exposed beyond the mound is a thin and extensive sheet of fine to medium ash from the eruption which shows pervasive climbing-ripple cross lamination. Interestingly, both the cross-lamination in this ash sheet where exposed west and north of the mound, and local crossbeds in coarse ash and lapilli ash beds of the mound itself, indicate deposition from currents flowing southward. As was recognized by Custer (1973), this direction indicates that glacially-fed bottom currents controlled transport directions; he concluded that ash was delivered by fall from a subaerial ash plume to the water, where it was entrained in the thermal density currents. It is inferred that these bottom currents redirected eruption-fed turbidity currents even during growth of the mound.redistributed downslope into the lake prior to deposition. The subcircular form of the mound is somewhat surprising given the apparent vigor of these currents, but this may be in part an artifact of erosion on the lakeward side of the edifice (which would have been the direction of elongation resulting from current redirection) and large-scale slumping to the north. Further work is underway to better understand development of this fascinating volcano.

Many subglacial eruptions produce deposits sharing many of the characteristics of those forming the Pahvant Butte and Black Point mounds. Recent work in Antarctica has shown that important parts of intraglacial and subglacial volcanoes are formed of waterlain tephra deposited from high-concentration and dilute turbidity currents, and from related density-modified grainflows, or cohesionless debris flows (Skilling, 1994; Smellie and Hole, 1997). Smellie and Hole (1997) recognize eruption-fed currents as the major process forming a lithofacies association dominated by 'poorly stratified gravelly sandstone', and further utilize aspects of deposit character to infer eruptive style. The use of sedimentary terminology for the deposits [which are 'lapilli tuffs' under the terminology of Schmid (1981) or Fisher and Schmincke (1984)] somewhat obscures the well-founded interpretation as eruption-fed flows, because such terms are more typically applied to deposits of turbidity currents formed from slumping of unstable fall deposits (Cas et al., 1986), as should be the term 're-sedimented syn-eruptive tephra (sensu McPhie et al., 1993)', but they may equally well be interpreted as eruption-fed turbidities. These subglacial volcanoes seem likely to have been constructed largely by eruption-fed aqueous density currents, particularly the parts of the volcanoes that formed during fully subaqueous phases of eruption.

Eruption-fed aqueous density currents also are inferred to have formed during the historic eruption of Myojinsho volcano off the coast of Japan, which has recently been re-analysed by Fiske et al. (1998). Little information is available on the bedding style of the volcano's deposits, but volcano bathymetry shows extremely even, radially sloping flanks that are inferred to have formed from high-particle concentration gravity flows developed from eruption-fed dense aqueous suspensions The steep, c. 20°, slopes of Myojinsho's flanks (and thus dip of the beds constituting the cone) suggest very inefficient transport, with high-particle-concentration currents moving essentially as aqueous grainflows in which interparticle collision and hindered settling, rather than turbulence,

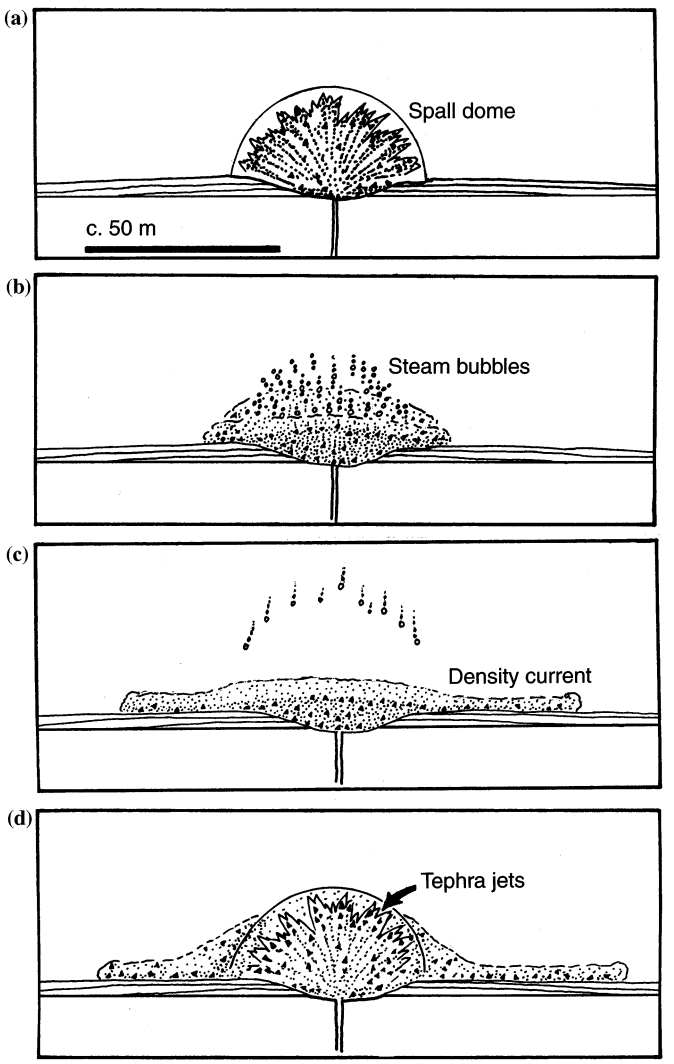

Fig. 6. Illustration of tephra-jetting activity feeding dilute eruption-fed turbidity currents. (a) Initial steamy tephra jets advance within accompanying subspherical spall dome generated by phreatomagmatic explosion(s). (b) Bubbles rise from collapsed spall dome, and tephra jets condense to release tephra particles into water column. (c) Tephra particles settle en masse, entraining water and forming laterally moving turbidity currents. (d) Succeeding eruptive pulse generates new tephra jet and spall dome, re-ejects material from vent and expands behind and beneath the turbidity current. Pressure waves are also associated with each explosion, passing through the surroundings well beyond the limits of the spall dome (after White, 1996).

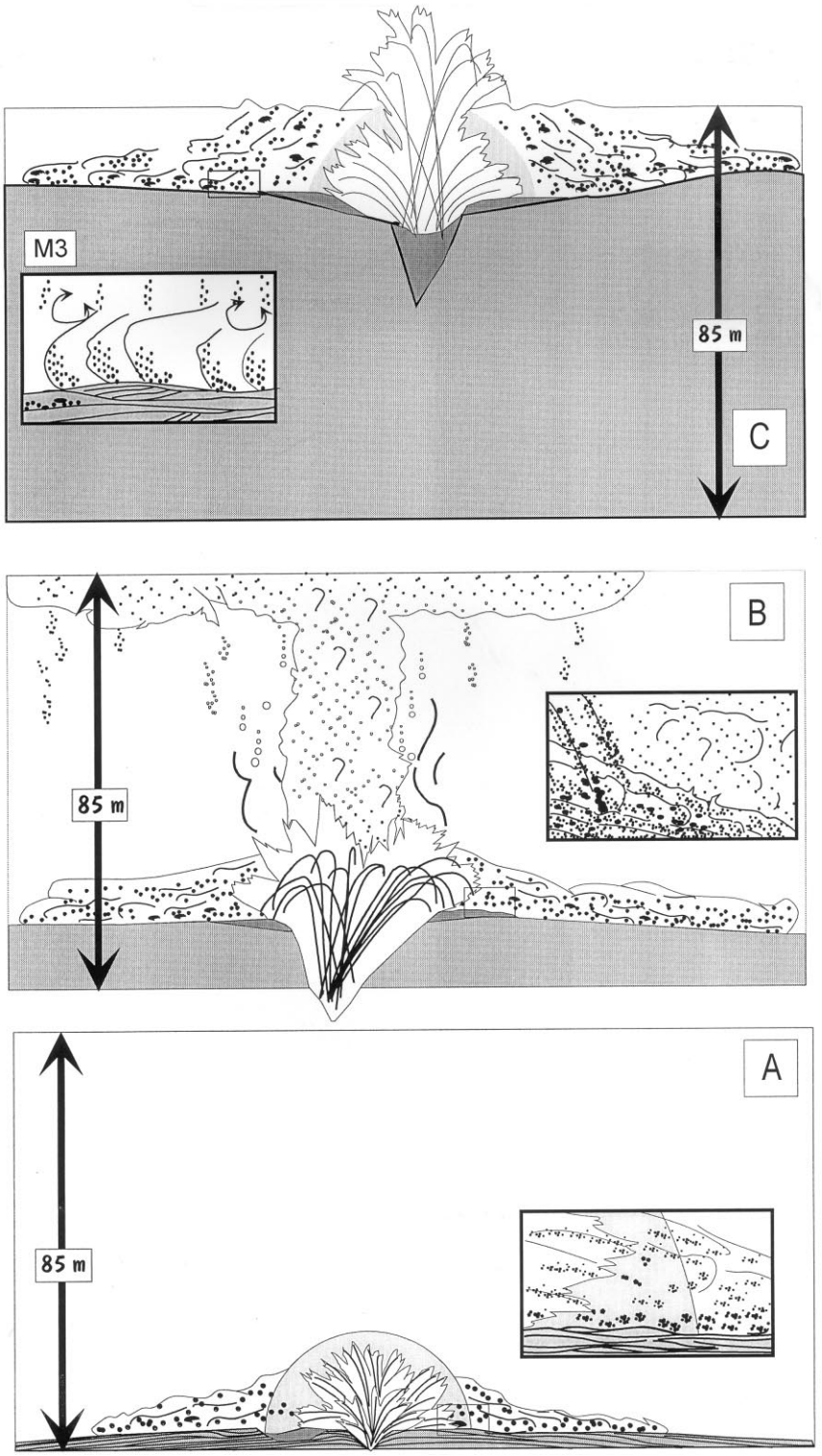

Fig. 7.

were the major grain support mechanisms (Nemec, 1990). Eruptive activity recorded by the flank deposits took place at shallow levels, with tephra jets venting to the surface. It was material stripped from the subaqueous jet margins and fallback from jets that fed the dense aqueous suspensions which evolved into flank-forming gravity currents. This contrasts with direct injection of tephra jets into the water column, as at Pahvant Butte and Black Point, which much more effectively disperses ejecta into the water and produces dilute eruption-fed aqueous density currents rather than hyperconcentrated ones as indicated for construction of Myojinsho's cone.

3.1. Recognition of Group II deposits

Deposits of eruption-fed aqueous density currents may show the entire range of sedimentary structures exhibited by grainflow deposits, debris flow deposits, and high- and low-concentration turbidites, so distinguishing eruption-fed sequences from products of immediately post-eruptive redeposition may not always be possible. Distinction of current-emplaced beds from subaqueous suspension-fall beds can be made on the basis of bed lenticularity, scouring, clast imbrication and cross-stratification, none of which will be present in the latter (Table 2). Key features of eruption-fed aqueous density flow deposits include their componentry, which will be entirely derived from the eruption itself. An absence, or minimal amount, of grain abrasion commonly allows preservation of clasts with complex shapes the deposits (Doucet et al., 1994; Fig. 10). Heat retention features may be associated with larger clasts (Mueller et al., 1993), but not with matrix clasts. Where original morphology can be reconstructed subaqueous edifices will be constructed largely of eruption-fed deposits, which are the primary deposits of the subaqueous realm. Consistent gradation in bedding style through a sequence of turbidites consisting of unabraded juvenile grains is likely to reflect evolution of an eruption (e.g. BTL 1b of Cousineau, 1994). Surt-

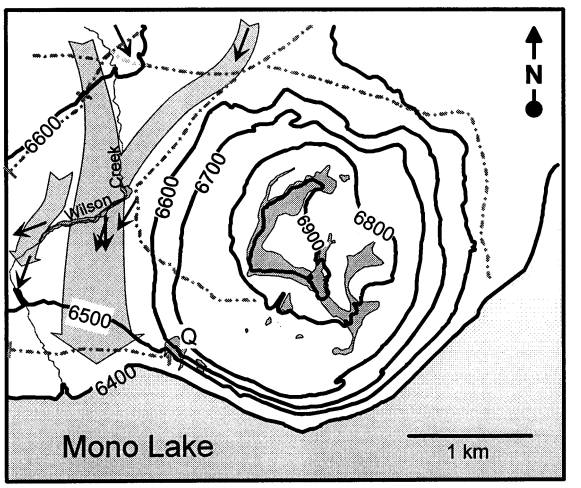

Fig. 8. Paleocurrent pattern of fine-grained eruption-fed density flow deposits at Black Point volcano, Mono Lake, eastern California. Paleocurrent arrows are from Custer (1973) and author's unpublished data, and are directed down the general paleolakefloor gradient rather than radially outward from the volcano. This pattern results from interaction of glacier-fed thermal underflows with eruption-fed turbidity currents ± fallout ash settling through the water column (Custer, 1973), and emphasizes different ways of generating eruption-fed sedimenting density flows, and the importance of any ambient currents in controlling local depositional features.

Fig. 7. Diagram illustrating mound growth at Pahvant Butte. Top and bottom of each frame represent lake surface and lake floor. (a) Early, fully subaqueous jetting activity. Explosions and collapsing jets produce a turbulent, dilute gravity flow having strong temperature contrasts and moving unsteadily outward from the vent. Deposition takes place largely from traction under unsteady flow conditions, but occasional ejection of the vent slurry or collapse of unusually concentrated tephra jets forms high-concentration dispersions that deposit massive beds. (b) Mound (stipple) is shallowing. Vigorous, more-sustained activity produces local and ephemeral water-exclusion zones at vent margin in which clasts are transported through an eruption-generated volatile pocket. This results in deposition of armored lapilli and tachylitic clasts having impact sags. (c) Mound has now grown into shallow water (asterisks denote 20 m wavebase). Jets are intermittently emergent. Turbidity currents carrying tephra outward along the mound surface interact with oscillatory currents beneath ambient lake surface waves and longer wavelength concentric waves induced by the eruption to produce combined-flow bedforms and cross-stratification of the M3 lithofacies (after White, 1996).

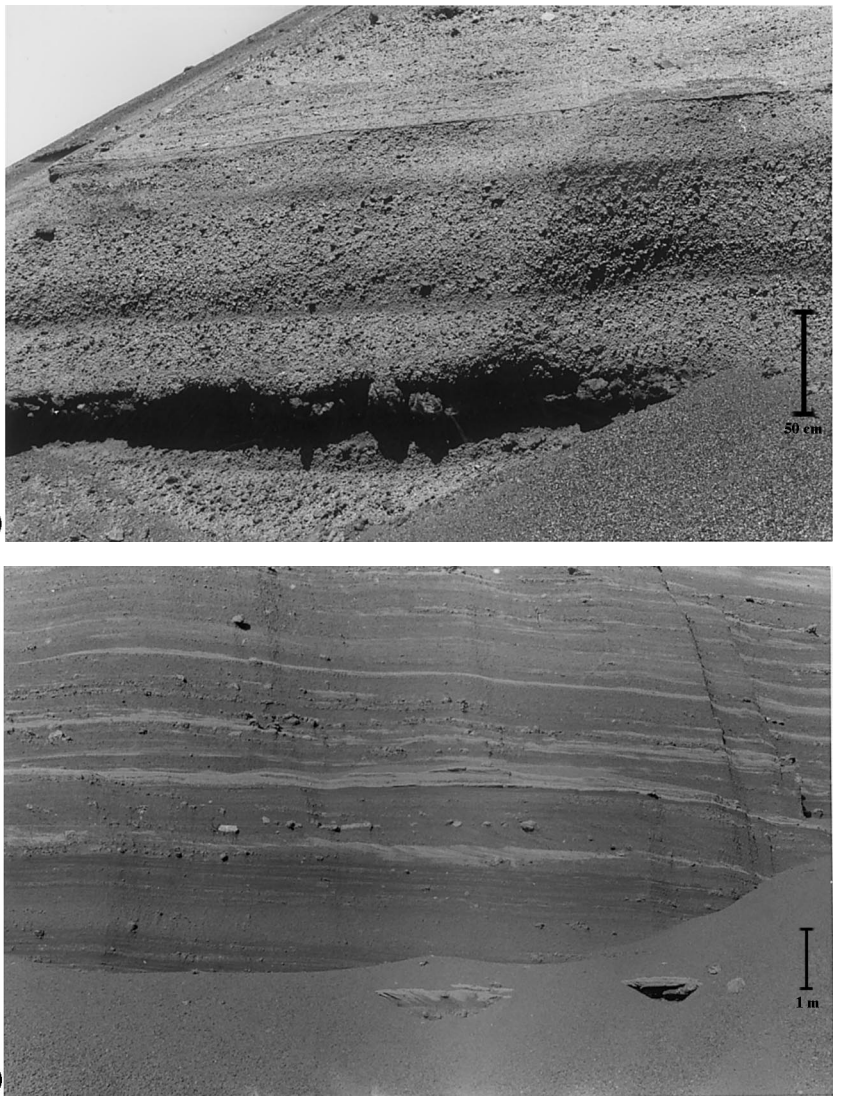

Fig. 9. The Black Point subaqueous mound strata share the low depositional dips of Pahvant Butte deposits, but exposed strata are less well bedded and lack recognizable combined-flow bedding features (cf. M3). (a) Subhorizontal beds of lapilli ash locally contain lenses of cauliflower bombs at the broadly scoured bases of thick beds. Bedding is defined by thin zones of lapilli-poor medium ash; some beds have reverse-graded bases; larger clasts locally occur isolated near the tops of beds. (b) Illustrated face is oriented $\sim$N–S at 'Q' (Fig. 8), and shows generally parallel bedding with subtle low-angle erosional surfaces, isolated cauliflower bombs and blocks of lake sediment (arrowed). A cross-stratified bed up to 40 cm thick extends across the photo, with foresets dipping to the right-tangential to the mound outline at this site, and downslop toward Mono Lake. (c) Beyond the mound an extensive deposit of fine-medium ash, up to 15 m thick, shows ubiquitous ripple-drift cross-lamination directed generally southward (Fig. 8). Ripple-drift horizons vary from a few cm thick, separated by thin planar beds of coarse ash or, rarely, lapilli, to 50 cm. (d) The lower contact of the ripple-drift unit sharply overlies pre-eruption lacustrine sediment. No lacustrine mud interbeds occur within the unit, and it is overlain by lacustrine sediment above a <1 m thick zone in which a few ash beds are intercalated.

seyan deposits of Bridge Point, New Zealand show an upward change to beds containing abraded clasts and fossils (Cas et al., 1989), and thus illustrate how associated facies and evidence for significant depositional hiatuses can be used to delimit sequences of eruption-fed deposits.

4. Group III: lava-fed density currents

This group includes turbidity currents and related non-turbulent flows such as grainflows, and grainfalls, which entrain and distribute particles formed and shed along the margins of advancing subaqueous lava flows (Table 3). Fragments are formed along the flow margins by thermal shock granulation, dynamo-thermal spalling or, above the critical depth for seawater (ca. 4200 m), localized and variably suppressed steam explosions. Ongoing fragmentation along the surfaces of advancing lava may result in development of a hyaloclastite carapace, maintained as a granular dispersion expanded by steam or buoyant hot water and jostled and penetrated by the lava. Advance of pillow tubes and buds generates minor fragmental debris, but more complex, rapid and irregular advance of fluidal lavas can result in greater degrees of fragmentation. Entrainment of fragments into density currents is aided by heating of the surrounding water along the flow margins

Fig. 9. (*Continued*)

Table 2
Summary information for eruption-fed aqueous density current deposits (Group II)

Feature	Inference	Interpretation
Homogeneous particle population, unabraded or very nearly so; complex clasts may be present; large clasts may show heat retention features	Homogeneous source, limited transport	Particles fed directly from erupting vent, in contrast to post-eruptive deposits that may incorporate other debris, involve interim stage of particle abrasion, e.g. from waves transport in water, large clasts self-insulated by steam films
Variable grainsize, often dominated by lapilli size	Variably effective fragmentation, fines either sorted out or not produced during eruption	Often from intermittent eruptions of Surtseyan or Strombolian style; fines may be winnowed from convective aqueous columns, margins of tephra jets
Thin to thick bedding, poor to good sorting, may show tractional bedforms	Non-sustained, multiple currents, sorting prior to current initiation and/or sorting during current transport	Originated by injection of tephra into water column, with nature of resulting currents controlled largely by initial suspended concentrations and particle populations
No matrix welding	Most fragments deposited cold	Particles cooled prior to or during aqueous transport; large particles may retain heat, but not sufficient to produce gas-phase flow

which generates convecting steam along flow margins and heated water which, as observed by Moore et al. (1973), produces significant rising currents above advancing subaqueous lava flows. These currents can entrain and loft small flow-generated hyaloclastite particles; the coarsest entrained particles may settle individually to form localized fall deposits. Finer particles are inferred to accumulate in suspension to feed initially vertical, low-energy, density currents which subsequently move downslope along the seafloor. Larger blocks forming as lava fragments on steep slopes commonly slide, roll and saltate downslope as debris falls (Nemec, 1990; Sohn et al., 1997). Conceptually, deposits of lava-fed density currents (LDCs) are distinct from those resulting from entirely post-eruptive redistribution of clasts by failure-generated turbidity currents or other mass flows, though in practice it is typically very difficult to demonstrate unambiguously a directly lava-fed origin.

Basaltic hyaloclastite some 200 m thick in south Iceland is inferred by Bergh and Gudmunder (1991) to have been deposited from lava flow-fed

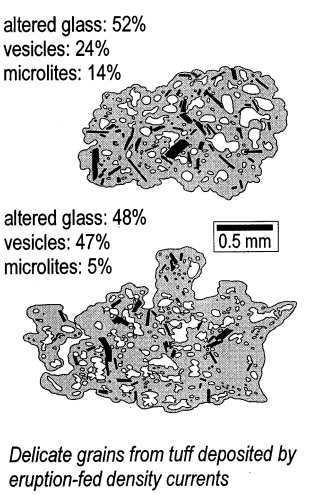

Fig. 10. Complex clast shapes in Archean tuff representing eruption-fed density current deposits (modified from Doucet et al., 1994). The consistency of the clast population, characterized by high glass content, moderate vesicularity, and clasts having unabraded highly re-entrant margins, argues against a reworked sedimentary origin for these beds.

Table 3
Summary information for lava flow-fed density current deposits (Group III)

Feature	Inference	Interpretation
Fragment shapes include blocky fragments, platy shards, sometimes 'limu' or hairlike shards; large proportions of fine fragments (smaller than 4 phi) are uncommon	Range of fragmentation processes form the shards; blocky and platy shards from thermal shock and dynamo-thermal spalling; 'limu' and hairlike shards from bursting and spattering of fluid lava	Lava flows fragment by chilling and stressing, and by local steam (or superheated water?) interactions; little fine ash produced
Weakly normal-graded beds, platy and 'limu' shards at tops of beds, local weak scouring, imbrication; some beds may be reverse graded	Deposition according to fall velocity, with indications of current activity, traction transport	Deposition from dilute sediment gravity flows
Pillow fragments, parapillows, isolated pillows with sand-grade matrix (sparse to supporting)	Poor sorting, mixing of clasts formed by different fragmentation processes	'Avalanching' of debris, as on lava delta foresets, steep slopes

density currents of both high and low particle concentrations stemming from subaqueous eruptions at shelfal depths. They envisage a high-flux eruption of basaltic magma that disintegrated upon contact with water into a weakly stratified mixture of fluidal coherent lava, lava rags, and quench-fragmented glass that flowed downslope from the eruption site. Upper parts of this mixture moved as a granular flow (aided by hot, buoyant interstitial water) that interacted with the underlying granular flow, and even with penetrating lava apophyses, to form weakly stratified beds with lava stringers. Entrainment of additional water along the top of the granular flow fostered turbidity currents, the deposits of which consist of well-defined graded beds that gradationally overlie the weakly stratified underlying hyaloclastite to complete what Bergh and Gudmunder (1991) termed the 'Standard Depositional Unit' for this sort of lava-fed hyaloclastite sequence (Fig. 11).

Bedded hyaloclastite occurring as thin sheetform deposits on modern seamounts has been inferred by Batiza et al. (1984) and Smith and Batiza (1989) to have been deposited by density currents. These deposits consist of beds centimeters to a couple of decimeters thick made up of glassy, non-vesicular, sideromelane fragments of two distinct shapes. The bulk of such deposits consists of blocky fracture-bounded grains typical of those formed by quench granulation (Carlisle, 1963) and shattering of thin rigid glass rinds as a result of movement in the fluid lava core (Kokelaar, 1986). Among these, however, are unusual fluidal fragments of the types referred to as Pele's hair and Pele's skin (limu o' Pele), the latter being most common and occurring as tiny (several mm^2) folded and recurved sheets. A recent re-examination by Batiza et al. (1996) of such deposits on Seamount Six suggests that these hyaloclastite fragments are formed by interaction of exceptionally fluid glassy lava with sediment and water, and that the sheetform bedded hyaloclastite deposits were deposited from lava flow-fed density currents. Details of this process are provided by Maicher (1999), but in outline the process envisaged involves entrapment of water or water-laden sediment within very thin, fast, flows of fluid lava. The deposits formed at water depths of c. 1800 m, somewhat above the critical depth for seawater, and it is inferred that the entrapped water boiled, expanding by a factor of perhaps $10\times$ to inflate and burst small bubbles that are represented by the limu fragments (Batiza et al., 1998; Maicher, 1998). The 'limu' together with blocky fragments simultaneously generated by quenching and dynamic shattering, arewere collected, entrained and lofted by steam and buoyant hot water along the lava flow, then dispersed locally downslope by weak, dilute density currents (Fig. 12).

A final environment, transitional from subaerial to subaqueous, in which density flows may be directly fed by advancing lava flows is on the foreset faces of lava deltas (Fuller, 1931; Moore et al., 1973). In this setting, fluidal lava is frag-

mented largely at the leading edge of the delta topset, with the fragments then accumulating as prograding avalanche faces by grainflow, grainfall and turbidity current processes (Nemec, 1990; Porebski and Gradzinski, 1990). Some coherent lava tubes make their way onto the foreset, where fragmentation continues to generate hyaloclastite, severed lava rags and pillow debris that are carried directly downslope by the same processes as outlined for the previous two settings, with finer-grained debris settling locally or being carried in dilute turbulent currents, and coarse blocks travelling downslope in debris falls. Additional detail is not presented for this transitionally-subaqueous case here, but extensive studies of lacustrine, glacial and modern settings are available (Fuller, 1931; Swanson, 1967; Jones, 1969; Moore et al., 1973; Skilling, 1994; Werner et al., 1996; Smellie and Hole, 1997).

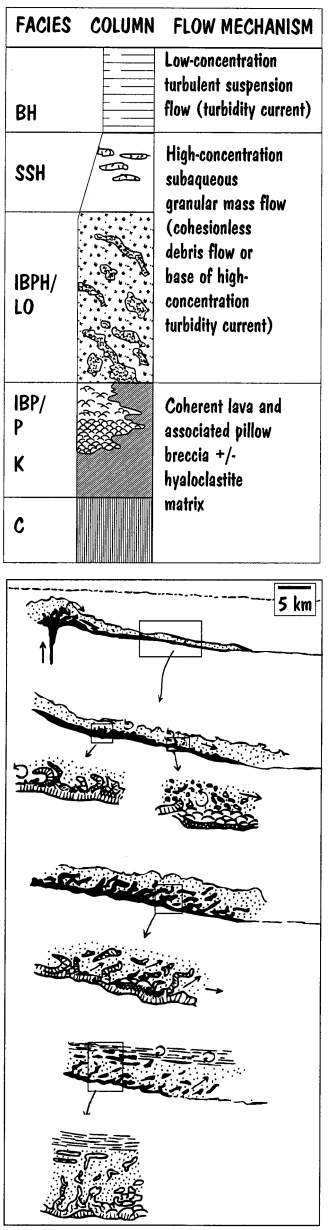

Fig. 11.

4.1. Recognition of lava-fed density current deposits

Where good lateral continuity of exposure exists, the deposits of lava-fed density currents will be clearly associated with simultaneously emplaced lava flows. The flows may be thin and glassy, and often show complex relationships with

Fig. 11. Model for production and summary of deposit features for thick lava-fed density current deposits formed on the Iceland shelf (from Bergh and Gudmunder, 1991). Top frame summarizes a representative depositional unit from a single eruptive event. BH = bedded hyaloclastite (multiple normally graded beds, small- and large-scale crossbedding, good sorting, alignment bedding); SSH = sideromelane shard hyaloclastite (high matrix and shard content, local lenses of fragmented basalt, vesicular and concavo-convex grains); IBPH/LO = isolated broken pillow hyaloclastite basalt/lobate basalt hyaloclastite breccia (poorly sorted, internally structureless, $>20\%$ matrix, large basalt lobes isolated within matrix, aligned and flow-folded basalt injections, infills topographic depressions, polyhedral clast shapes); IPB/P = isolated pillow breccia/pillow basalt (isolated pillows with $<20\%$ matrix, close-packed pillows and pillow tubes, circular and ellipsoid lava shapes, textural zoning); K = cube-jointed basalt (irregular jointing, compact lobes, rotated basalt slivers, fanning-rosette columnar jointing; C = regular columnar jointed basalt (regular columns, extensive unit). Lower frame illustrates the processes envisaged to produce such deposits, which include (note scales) thermal, dynamothermal and mild phreatomagmatic disruption of subaqueously erupting magma, movement of high-concentration sediment gravity flows away from the vent simultaneously with seafloor advance of fluid lava, complex mingling of gravity flow deposits with fluid lava, and evolution of dilute turbidity currents carrying material stripped from the top of the high-concentration flow.

the hyaloclastite. Deposits of LDCs may include a range of broadly autoclastic fragments including glassy curved splinter shards and blocky shards, parapillows (Walker, 1992), and pillow fragments (Table 3), which may be segregated into coarse debris-fall deposits and finer-grained turbidites and lava-marginal fall deposits. Fine ash is not an important component because few fine-ash grade fragments are formed by autoclasis (McPhie et al., 1993). Fluidal sideromelane fragments are uncommon, and where present indicate weakly explosive interaction of fluidal lava flows with ambient or sediment hosted water.

5. Related deposits: column-margin fall

Associated with eruption-fed subaqueous density current deposits beyond the vent area are (a) 'normal' sedimentary deposits, either background ones (e.g. pelagic ooze) or those from remobilization and redeposition of tephra from eruption-fed deposits; (b) aqueous fallout deposits, which may be derived from subaerial or subaqueous eruption plumes, and in some cases; (c) lava flows or shallow intrusions. At the margins of a subaqueous vent, an additional type of deposition may take place out of eruption columns from which water is excluded by magmatic volatiles. These deposits form in subaqueous settings within vents or on their margins, yet show no evidence of interaction with water. Kokelaar (1983) termed such water-exclusion zones 'cupolas', and described evidence from Surtla for clast agglutination on impact which he interpreted to support the existence of a water-excluded zone during that entirely subaqueous eruption. One facies at Pahvant Butte has similarly been interpreted to have formed in a zone of water exclusion on the basis of position near the base of the volcano, local distribution, and presence of impact sags, armoured lapilli and accretionary lapilli (White, 1996). In both cases, the phenomenon of water exclusion is inferred to be associated with continuous eruption. Rheomorphically welded ignimbrite, similarly inferred to have formed in a water-excluded zone in a rhyolitic vent is discussed by Kano et al. (1997), Schmincke and Bednarz (1990) identify subaqueously formed spatter agglutinate in the deep-water Troodos Ophiolite, and Gill et al. (1990) describe tack-welded scoria from the modern seafloor of the Sumisu Rift. All of these units are inferred to have formed by fallout or very localized flow at high depositional rates and particle concentrations, in or at the margins of vents. Although not themselves generally products of subaqueous density currents, study of such deposits can provide important ancillary information to reconstruct the evolution of an eruption responsible for a suite of density current deposits. Cas and Wright (1991) infer that some rocks interpreted as subaqueously welded ignimbrite are the result of this sort of process, and that they should not be considered pyroclastic flow deposits.

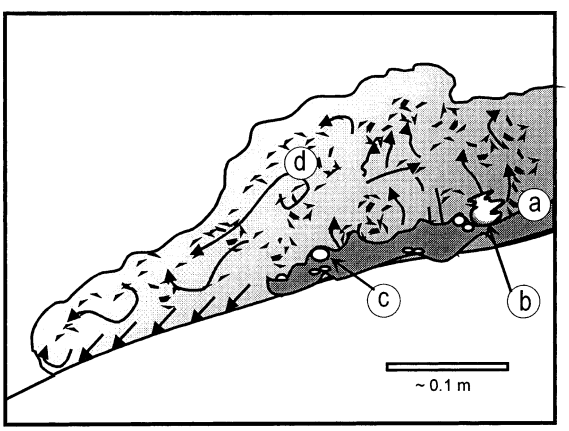

Fig. 12. Schematic illustration of processes resulting in limu-bearing sheet hyaloclastite at c. 2 km water depth. Four aspects of note are (a) spalling and thermal granulation of advancing lava form blocky, poorly or nonvesicular sideromelane shards; (b) water entrapped beneath the front of rapidly advancing thin, glassy lava flow expands to form bubbles which burst, yielding limu fragments; (c) steam forms and flows along lava-flow margins, and hot water rises vigorously from flow, lofting fragments above the seafloor to form a particulate dispersion; (d) excess density of the dispersion results from particle accumulation or heat loss, resulting in dilute vertical sediment-gravity flows which encounter the seafloor and runout downslope.

Table 4
Summary information for column-margin fall deposits formed in water-excluded zones

Feature	Inference	Interpretation
Diffuse or parallel bedding contacts; local normal grading	Absence of current during deposition (no traction features)	Suspension/fall deposition
Local bomb or block sags	Ballistic impact sags	Ballistic transport in gas (rather than liquid) medium
Tachylite or microcrystalline clasts; little or no sideromelane; welded clasts or matrix with uniform paleomagnetic signature	Heat retention features, indicative of emplacement at high temperature	Pyroclasts not in contact with water prior to deposition
Local armoured lapilli (and/or core-type accretionary lapilli?)	Accretion of damp ash to form aggregate grains	Transport as dispersed particles in droplet-laden gas; pyroclasts not enclosed in water during particle accretion

5.1. Recognition of column-margin fall deposits

Key indicators of column-margin water-exclusion zones are heat-retention features, such as welding and clast agglutination, and accretionary textures such as armoured lapilli (Table 4). Evidence of heat retention by small clasts is especially important — larger clasts may evolve their own steam carapaces or exclusion zones because of their relatively great heat content, but small clasts are rapidly chilled and cannot retain significant heat if dispersed in water. Agglutination of clasts or welding of vitric ash are diagnostic, though McPhie and Hunns (1995) offer a cautionary discussion of a tuff welded subaqueously by later hypabyssal intrusion of basalt. Accretionary textures typically form where water vapor facilitates adhesion of small grains, and do not form in the presence of excessive water (Schumacher and Schmincke, 1995), such as where tephra grains are entrained in water. Similarly, well developed block and bomb sags require high impact velocities resulting from ballistic transport, and do not occur where clasts fall to the depositional site through water.

6. Concluding comments

Deposits of eruption-fed subaqueous density currents are likely to be far more common than has been recognized to date. This assertion rests primarily on the observation that during subaqueous eruptions, large quantities of debris are introduced rapidly into the water column above the depositional surface. Settling of masses of particles is fundamentally different from settling of individual particles (Bradley, 1965; Allen, 1982; Carey et al., 1988; Druitt, 1995; Fiske et al., 1998), and forms vertical sediment gravity flows that flow downward to the substrate where they are redirected laterally. At the highest eruption rates, subaqueous currents may show much the same behaviour as subaerial ones because water is excluded from both the column and substantial parts of the resulting current. Intermediate eruption rates result in water being excluded only locally from the vent region, and it is drawn convectively into the column as erupting volatiles condense or separate from the particles (Kokelaar, 1986; Kano et al., 1996). Collapse of all or part of such a convecting mass of water and tephra may feed high particle concentration density currents initially, with subsequent pulses becoming increasingly dilute. Where eruption is intermittent, such as Surtseyan jetting (or Strombolian bursts), condensation of jet volatiles and steam leaves a stream of tephra spread through the water, typically generating dilute turbidity currents (White, 1996). Even particles generated along subaqueous lava flows may directly feed density currents if they are carried into the water by thermal convection, though significant transport is likely only on substantial slopes.

References

Allen, J.R.L., 1982. Sedimentary Structures. Their Character and Physical Basis. Developments in Sedimentology, 30. Elsevier, Amsterdam, 593 pp.

Aramaki, S., 1957. Classification of pyroclastic flows (in Japanese). J. Volcanol. Soc. Jpn. 1 (series 2), 47–57. English Translation (1961), International Geology Review 3, 518–524.

Aramaki, S., Yamasaki, M., 1963. Pyroclastic flows in Japan. Bull. Volcanol. 26, 89–99.

Arnott, R.W.C., Hand, B.M., 1989. Bedforms, primary structures and grain fabric in the presence of supended sediment rain. J. Sed. Petrol. 59, 1062–1069.

Batiza et al., 1996. New evidence from Alvin for the origin of deep-sea eruptive hyaloclastite on Seamount 6, Cocos Plate, 12°43′ N. 1995 Fall Meeting Abstracts, EOS, 76: F650.

Batiza, R., Coleman, T., White, J., Pan, Y., 1998. Deep Sea Hyaloclastites: new data from Alvin and laboratory studies. In: Geological Society of America Penrose conference on evolution of ocean islands, Program and Abstracts: 18.

Batiza, R., Fornari, D.J., Vanko, D.A., Lonsdale, P., 1984. Craters, caldereas and hyaloclastites on young Pacific seamounts. J. Geophys. Res. 89, 8371–8390.

Bergh, S.G., Gudmunder, E.S., 1991. Pleistocene mass-flow deposits of basaltic hyaloclastite on a shallow submarine shelf, South Iceland. Bull. Volcanol. 53, 597–611.

Bradley, W.H., 1965. Vertical density currents. Science 150, 1423–1428.

Branney, M.J., Kokelaar, B.P., 1992. A reappraisal of ignimbrite emplacement: progressive aggradation and changes from particulate to non-particulate flow during emplacement of high-grade ignimbrite. Bull. Volcanol. 54, 504–520.

Busby-Spera, C.J., 1986. Depositional features of rhyolitic and andesitic volcaniclastic rocks of the Mineral King submarine caldera complex, Sierra Nevada, California. J. Volcanol. Geotherm. Res. 27, 43–76.

Campbell, C.S., 1990. Rapid granular flows. Ann. Rev. Fluid Mech. 22, 57–92.

Carey, S.N., Sigurdsson, H., Sparks, R.S.J., 1988. Experimental studies of particle-laden plumes. J. Geophys. Res. 93, 314–328.

Carlisle, D., 1963. Pillow breccias and their aquagene tuffs, Quadra Island, British Columbia. J. Geol. 71, 48–71.

Cas, R.A.F., Landis, C.A., Fordyce, R.E., 1989. A monogenetic, Surtla-type, Surtseyan volcano from the Eocene-Oligocene Waiareka-Deborah volcanics, Otago, New Zealand: a model. Bull. Volcanol. 51, 281–298.

Cas, R.A.F., Landis, C.A., Kawachi, Y., Fordyce, R.E., 1986. The Eocene-Oligocene Oamaru volcano: an outstanding facies model for surtseyan volcanoes; possible base surges, and the importance of comtemporaneous epiclastic processes.

Cas, R.A.F., Wright, J.V., 1987. Volcanic Successions, Modern and Ancient. Allen and Unwin, London, 528 pp.

Cas, R.A.F., Wright, J.V., 1991. Subaqueous pyroclastic flows and ignimbrites: an assessment. Bull. Volcanol. 53, 357–380.

Christensen, M.N., Gilbert, C.M., 1964. Basaltic cone suggest constructional origin of some guyots. Science 143, 240–242.

Cousineau, P.A., 1994. Subaqueous pyroclastic deposits in an Ordovician fore-arc basin: An example from the Saint-Victor Formation, Quebec Appalachians, Canada. J. Sed. Res. Section A Sed. Petrol. Proc. 64, 867–880.

Custer, S.G., 1973. Stratigraphy and Sedimentation of Black Point Volcano, Mono Basin, California. M.S. Thesis, University of California at Berkeley, 114 pp.

Doucet, P., Mueller, W., Chartrand, F., 1994. Archean, deep-marine, volcanic eruptive products associated with the Coniagas massive sulfide deposit, Quebec, Canada. Can. J. Earth Sci. 31, 1569–1584.

Druitt, T.H., 1995. Settling behaviour of concentrated dispersions and some volcanological applications. J. Volcanol. Geotherm. Res. 65, 27–39.

Fisher, R.V., Schmincke, H.-U., 1984. Pyroclastic Rocks. Springer-Verlag, Berlin, 472 pp.

Fiske, R.S., 1963. Subaqueous pyroclastic flows in the Ohanapecosh Formation, Washington. Geol. Soc. Am. Bull. 74, 391–406.

Fiske, R.S., Matsuda, T., 1964. Submarine equivalents of ash flows in the Tokiwa Formation, Japan. Am. J. Sci. 262, 76–106.

Fiske, R.S., Cashman, K.V., Shibata, A., Watanabe, K., 1998. Tephra dispersal from Myojinsho, Japan, during its shallow submarine eruption of 1952–1953. Bull. Volcanol. 59, 262–275.

Freundt, A., 1998. The formation of high-grade ignimbrites, I: experiments on high- and low-concentration transport systems containing sticky particles. Bull. Volcanol. 59, 414–435.

Freundt, A., Schmincke, H.-U., 1995. Eruption and emplacement of a basaltic welded ignimbrite during caldera formation on Gran Canaria. Bull. Volcanol. 56, 640–659.

Fritz, W.J., Stillman, C.J., 1996. A subaqueous welded tuff from the Ordovician of County Waterford, Ireland. J. Volcanol. Geotherm. Res. 70, 91–106.

Fuller, R.E., 1931. The aqueous chilling of basaltic lava on the Columbia River Plateau. Am. J. Sci. 21, 281–300.

Gilbert, G.K., 1890. Lake Bonneville. U.S. Geol. Surv. Mon. 1, 1–438.

Gill, J., et al., 1990. Explosive deep water basalt in the Sumisu backarc rift. Science 248, 1214–1217.

Head, J.W., Wilson, L., 1989. Basaltic pyroclastic eruptions: influence of gas-release patterns and volume fluxes on fountain structure, and the formation of cinder cones, spatter cones, rootless flows, lava ponds and lava flows. J. Volcanol. Geotherm. Res. 37, 261–271.

Howells, M.F., Campbell, D.G., Reedman, A.J., 1985. Isolated pods of subaqueous welded ash-flow tuff: a distal facies of the Capel Curig Volcanic Formation (Ordovician), North Wales. Geol. Mag. 122, 175–180.

Jones, J.G., 1969. Intraglacial volcanoes of the Laugarvatn region, southwest Iceland. J. Geol. Soc. London 124, 197–211.

Kano, K., Orton, G.J., Kano, T., 1994. A hot Miocene subaqueous scoria-flow deposit in the Shimane Peninsula, SW Japan. J. Volcanol. Geotherm. Res. 60, 1–14.

Kano, K., Yamamoto, T., Ono, K., 1996. Subaqueous eruption and emplacement of the Shinjima Pumice, Shinjima (Moeshima) Island, Kagoshima Bay, SW Japan. J. Volcanol. Geotherm. Res. 71, 187–206.

Kano, K., Matsuura, H., Yamauchi, S., 1997. Miocene rhyolitic welded tuff infilling a funnel-shaped eruption conduit Shiotani, southeast of Matsue, SW Japan. Bull. Volcanol. 59, 125–135.

Kneller, B.C., Branney, M.J., 1995. Sustained high-density turbidity currents and the deposition of thick massive sands. Sedimentology 42, 607–616.

Kokelaar, B.P., 1983. The mechanism of Surtseyan volcanism. J. Geol. Soc. Lond. 140, 939–944.

Kokelaar, B.P., 1986. Magma–water interactions in subaqueous and emergent basaltic volcanism. Bull. Volcanol. 48, 275–289.

Kokelaar, B.P., Busby, C.J., 1992. Subaqueous explosive eruption and welding of pyroclastic deposits. Science 257, 196–201.

Lowe, D.R., 1976. Subaqueous liquified and fluidized sediment flows and their deposits. Sedimentology 23, 285–308.

Lowe, D.R., 1982. Sediment gravity flows: II. Depositional models with special reference to the deposits of high-density turbidity currents. J. Sed. Petrol. 52, 279–297.

Lowe, D.R., 1988. Suspended-load fallout rate as an independent variable in the analysis of current structures. Sedimentology 35, 765–776.

Maicher, D., 1998. Deep-sea 'limu o' Pelee' formation. In: International Volcanological Conference, Cape Town, South Africa, pp. 38.

Maicher, D., 1999. Hyaloclastite beds of shelf and seamount: roles of exsolution, entrapment and entrainment. Unpublished PhD dissertation Thesis, University of Otago, Dunedin, New Zealand, 272 pp.

Mandeville, C.W., Carey, S., Sigurdsson, H., King, J., 1994. Paleomagnetic evidence for high-temperature emplacement of the 1883 subaqueous pyroclastic flows from Krakatau Volcano, Indonesia. J. Geophys. Res. 99, 9487–9504.

McPhie, J., Doyle, M., Allen, R., 1993. Volcanic Textures: a guide to the interpretation of textures in volcanic rocks. CODES Key Centre, University of Tasmania, Hobart, 198 pp.

McPhie, J., Hunns, S.R., 1995. Secondary welding of submarine, pumice-lithic breccia at Mount Chalmers, Queensland, Australia. Bull. Volcanol. 57, 170–178.

Mohrig, D., Whipple, K.X., Hondzo, M., Ellis, C., Parker, G., 1998. Hydroplaning of subaqueous debris flows. Geol. Soc. Am. Bull. 110, 387–394.

Moore, J.G., Phillips, R.L., Grigg, R.W., Peterson, D.W., Swanson, D.A., 1973. Flow of lava into the sea 1969–1971, Kilauea Volcano, Hawaii. Geol. Soc. Am. Bull. 84, 537–546.

Mueller, W., White, J.D.L., 1992. Felsic fire-fountaining beneath Archean seas: pyroclastic deposits of the 2730 Ma Hunter Mine Group, Quebec, Canada. J. Volcanol. Geotherm. Res. 54, 117–134.

Mueller, W., Chown, E.H., Potvin, R., 1993. Substorm wave base felsic hydroclastic deposits in the Archean Lac des Vents volcanic complex, Abitibi belt, Canada. J. Volcanol. Geotherm. Res. 60, 273–300.

Nemec, W., 1990. Aspects of sediment movement on steep delta slopes. In: Colella, A., Prior, D.B. (Eds.), Coarse-Grained Deltas. Int. Assoc. Sed. Spec. Pub. 10, 29–73.

Nichols, R.J., Sparks, R.S.J., Wilson, C.J.N., 1994. Experimental studies of the fluidization of layered sediments and the fromation of fluid escape structures. Sedimentology 41, 233–253.

Orton, G.J., 1991. Emergence of subaqueous depositional environments in advance of a major ignibrite eruption, Capel Curig Volcanic Formation, Ordovician, North Wales-an example of regional volcanotectonic uplift? Sed. Geol. 74, 251–286.

Porebski, S.J., Gradzinski, R., 1990. Lava-fed Gilbert-type delta in the Polonez Cove Formation (Lower Oligocene), King George Island, West Antarctica. In: Coarse-Grained Deltas. Int. Assoc. Sed. Spec. Pub. 10, 335–351.

Postma, G., 1986. Classification for sediment gravity-flow deposits based on flow conditions during sedimentation. Geology 14, 291–294.

Postma, G., Nemec, W., Kleinspehn, K.L., 1988. Large floating clasts in turbidites: a mechanism for their emplacement. Sed. Geol. 58, 47–61.

Schmincke, H.-U., Bednarz, U., 1990. Pillow, sheet flow and breccia flow volcanoes and volcano-tectonic hydrothermal cycles in the Extrusive Series of the northeastern Troodos ophiolite (Cyprus). In: Malpas, J., Moores, E.M., Panayiotou, A., Xenophontos, C. (Eds.), Ophiolites, Oceanic Crustal Analogues: proceedings of the Symposium 'Troodos 1987'. Geological Survey Dept, Ministry of Agriculture and Natural Resources, Nicosia, Cyprus, pp. 185–206.

Schneider, J.-L., Fourquin, C., Paicheler, J.-L., 1992. Two examples of subaqueously welded ash-flow tuffs: the Visean of southern Vosges (France) and the upper Creatceous of northern Anatolia (Turkey). J. Volcanol. Geotherm. Res. 49, 365–383.

Schumacher, R., Schmincke, H.-U., 1995. Models for the origin of accretionary lapilli. Bull. Volcanol. 56, 626–639.

Skilling, I.P., 1994. Evolution of an englacial volcano: Brown Bluff, Antartica. Bull. Volcanol. 56, 573–591.

Smellie, J.L., Hole, M.J., 1997. Products and processes in Pliocene-Recent, subaqueous to emergent volcanism in the Antarctic Peninsula: examples of englacial Surtseyan volcano construction. Bull. Volcanol. 58, 628–646.

Smith, T.L., Batiza, R., 1989. New field and laboratory evidence for the origin of hyaloclastite flows on seamount summits. Bull. Volcanol. 51, 96–114.

Sohn, Y.K., 1997. On traction-carpet sedimentation. J. Sed. Res. 67, 502–509.

Sohn, Y.K., Kim, S.B., Hwang, I.G., Bahk, J.J., Choe, M.Y., Chough, S.K., 1997. Characteristics and depositional processes of large-scale gravelly Gilbert-type foresets in the Miocene Doumsan fan delta, Pohang Basin, SE Korea. J. Sed. Res. 67, 130–141.

Sparks, R.S.J., Sigurdsson, H., Carey, S.N., 1980. The entrance of pyroclastic flows into the sea, II. Theoretical considerations on subaqueous emplacement and welding. J. Volcanol. Geotherm. Res. 7, 97–105.

Swanson, D.A., 1967. Yakima basalt of the Tieton river area, south central Washington. Geol. Soc. Am. Bull. 78, 1077–1110.

Thorarinsson, S., 1967. Surtsey. The New Island in the North Atlantic. The Viking Press, New York, 47 pp.

Valentine, G.A., 1987. Stratified flow in pyroclastic surges. Bull. Volcanol. 49, 616–630.

Walker, G.P.L., 1992. Morphometric study of pillow-size spectrum among pillow lavas. Bull. Volcanol. 54, 459–474.

Werner, R., Schmincke, H.-U., Sigvaldason, G., 1996. A new model for the evolution of table mountains: volcanological and petrological evidence from the Herdubreid and Herdubreidarotgl volcanoes (Iceland). Geol. Rundsch. 85, 390–397.

White, J.D.L., 1994. Sublacustrine eruptive processes, Pleistocene Lake Russell, California, USA. Abstracts. Geol. Soc. New Zealand Ann. Conf. Geol. Soc NZ Misc. Pub. 80A, 186.

White, J.D.L., 1996. Pre-emergent construction of a lacustrine basaltic volcano, Pahvant Butte, Utah (USA). Bull. Volcanol. 58, 249–262.

White, M.J., McPhie, J., 1997. A submarine welded ignimbrite-crystal-rich sandstone facies association in the Cambrian Tyndall Group, western Tasmania, Australia. J. Volcanol. Geotherm. Res. 76, 277–295.

Wilson, C.J.N., 1980. The role of fluidization in the emplacement of pyroclastic flows: an experimental approach. J. Volcanol. Geotherm. Res. 8, 231–249.

Wohletz, K.H., Sheridan, M.F., 1983. Hydrovolcanic explosions II. Evolution of basaltic tuff rings and tuff cones. Am. J. Sci. 283, 384–413.